

## Highlighted Generation of Fluorescence Signals Using Simultaneous Two-Color Irradiation on Dronpa Mutants

Ryoko Ando,\* Cristina Flors,<sup>†</sup> Hideaki Mizuno,\* Johan Hofkens,<sup>†</sup> and Atsushi Miyawaki\*

\*Laboratory for Cell Function and Dynamics, Advanced Technology Development Group, Brain Science Institute, The Institute of Physical and Chemical Research, Hirosawa, Wako-city, Saitama 351-0198, Japan; and <sup>†</sup>Department of Chemistry, Katholieke Universiteit Leuven, 3001 Heverlee, Belgium

**ABSTRACT** Dronpa absorbs blue light and emits bright green fluorescence. It can also be converted by strong irradiation at 490 nm to a nonfluorescent state, which can then be switched back to the original emissive state with irradiation at 400 nm. Through semirandom mutagenesis studies, we have developed two mutants of Dronpa that show efficient photoswitching kinetics. Compared to Dronpa, the mutants can be turned off by blue light more efficiently. Thus, excitation with an argon laser line (488 nm) makes the mutants quickly become dark such that no substantial fluorescence signals can be observed. Excitation with a violet laser diode (405 nm) also produces no fluorescence signals. Simultaneous 488- and 405-nm irradiation, however, results in a rapid oscillation between the two states, thereby keeping the emissive state population large enough to produce sufficiently bright fluorescence signals.

Received for publication 5 February 2007 and in final form 12 March 2007.

Address reprint requests and inquiries to Atsushi Miyawaki, Tel.: 81-48-467-5917; Fax: 81-48-467-5924; E-mail: matsushi@brain.riken.jp.

Although Dronpa normally absorbs at 503 nm and emits green fluorescence with a high fluorescence quantum yield ( $\phi_{FL} = 0.85$ ), strong irradiation at 488 nm can convert this protein to a nonfluorescent state that absorbs at 390 nm (dark state (D)). The protein can then be switched back to the original emissive state (bright state (B)) with minimal irradiation at 405 nm (1–3). The conversion from the B state to the D state requires a large number of photons ( $\phi_{BD} = 0.0003$ ), whereas the D-to-B conversion occurs efficiently ( $\phi_{DB} = 0.37$ ). The photochromic characteristics of Dronpa provide an unprecedented molecular tool for studying fast protein dynamics at multiple time points in individual cells (1).

cDNA encoding Dronpa was subjected to an error-prone PCR. *Escherichia coli* cells transformed with plasmids carrying the mutagenized DNA were plated and screened for different photoswitching behavior using a home-made image analyzing system equipped with two xenon lamps (75 W and 300 W) (4). The plates were directly illuminated with intense blue ( $490 \pm 10$  nm) or violet ( $400 \pm 7.5$  nm) light emitted from the 300-W lamp. Colonies illuminated with weak blue light ( $490 \pm 10$  nm) from the 75-W lamp were examined for green fluorescence and imaged using a cooled charge-coupled device camera. Of  $\sim 1,000$  colonies, 6 colonies showing rapid photobleaching upon intense illumination at 490 nm were identified. Interestingly, all of these colonies quickly recovered their fluorescence after the intense 490-nm light was turned off. Sequence analysis of the Dronpa variants in these mutants revealed that each of them carried a mutation of either Val<sup>157</sup> or Met<sup>159</sup>. One of the mutant proteins, Dronpa-Met<sup>159</sup>Thr, was named Dronpa-2 and further characterized. In parallel, a degenerative primer was designed so that Val<sup>157</sup> and Met<sup>159</sup> would be randomly replaced with other amino

acids. Site-directed random mutagenesis of Dronpa generated a new mutant protein, which showed a more efficient spontaneous recovery of fluorescence after bleaching. This mutant, which was named Dronpa-3, carried two mutations: Val<sup>157</sup>Ile and Met<sup>159</sup>Ala.

The recombinant Dronpa-2 and Dronpa-3 proteins were expressed in *E. coli* and purified. The oligomerization states of these two mutants were examined using analytical equilibrium ultracentrifugation analysis; their molecular masses were determined to be 28 kDa (data not shown), which confirmed that they were monomers. Recombinant Dronpa, Dronpa-2, and Dronpa-3 were each placed in a droplet of mineral oil on a coverslip (Fig. 1). The time courses of the fluorescence intensities were monitored simultaneously from the three droplets using a 490DF20 excitation filter overlaid with a 0.5% transmittance neutral density (ND) filter, a 505DRLPXR dichroic mirror, and a 535DF25 emission filter. The droplets were continuously illuminated through a 50% transmittance ND filter at 490 nm (490DF20;  $0.40 \text{ W/cm}^2$ ) and 400 nm (400DF15;  $0.14 \text{ W/cm}^2$ ) to induce photobleaching and photoactivation during the intervals at the beginning and the end of the experiment, respectively. With the intense illumination at 490 nm, the fastest decrease in the fluorescence intensity was observed for Dronpa-2, whereas the slowest decrease was observed for Dronpa. In another experiment, using less intense 490-nm light resulted in more detailed decay curves for the three samples. In comparison to the quantum yield for the B-to-D conversion of Dronpa ( $3 \times 10^{-4}$ ) (1), the values ( $\phi_{BD}$ ) for Dronpa-2 and Dronpa-3 were

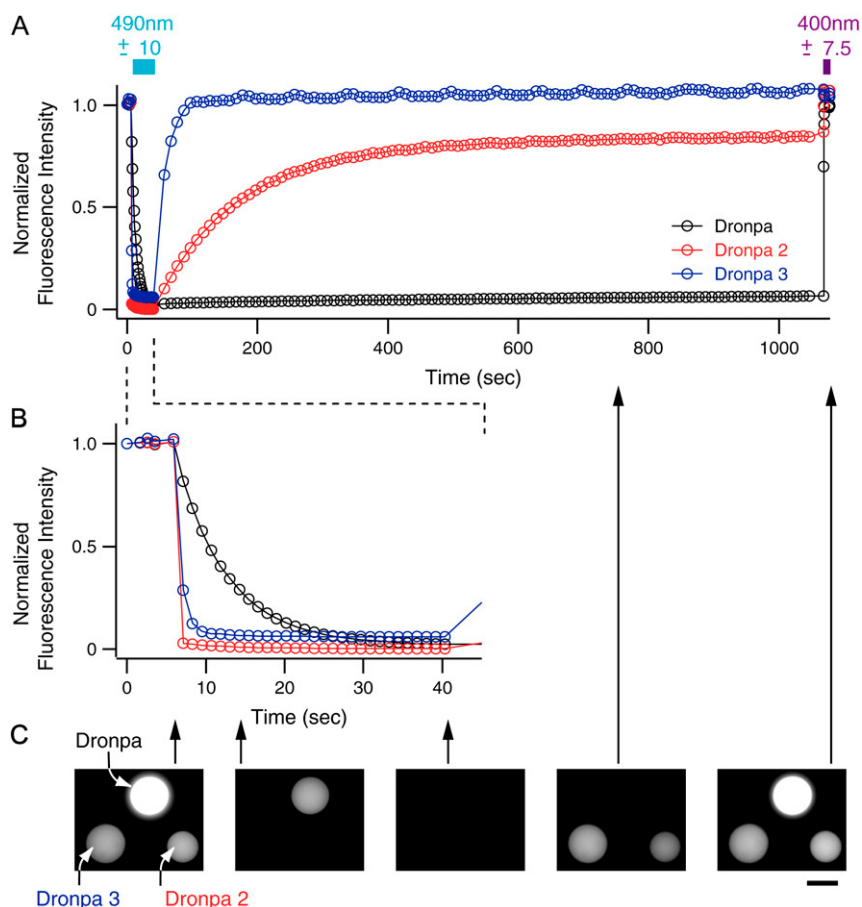


**FIGURE 1** Photochromic behaviors of Dronpa, Dronpa-2, and Dronpa-3. (A) Time courses of green fluorescence intensities of Dronpa (black), Dronpa-2 (red), and Dronpa-3 (blue) in droplets of mineral oil. Green fluorescence was monitored with a 490DF20 excitation filter overlaid with an ND filter, a 505DRLPXR dichroic mirror, and a 535DF25 emission filter. During the marked intervals (blue and violet bars), the droplets were continuously illuminated through an ND filter at 490 nm (490DF20) or 400 nm (400DF15) to induce photobleaching or photoactivation, respectively. (B) The same time courses as shown in (A) between 0 and 40 s on an expanded time scale. (C) Arrows above the first three panels indicate positions on the time scale in (B), whereas those above the last two panels indicate positions on the time scale in (A). Interference filters were obtained from Omega Optical (Brattleboro, VT).

calculated to be larger at  $4.7 \times 10^{-2}$  and  $5.3 \times 10^{-3}$ , respectively. Note that Dronpa-2 and Dronpa-3 quickly returned to their emissive states even in the dark, which contrasts with the stable dark state of Dronpa. Because of the apparent thermal instability of their dark states, the quantum yields for the D-to-B conversion by 400-nm light could not be measured for Dronpa-2 and Dronpa-3. These mutants, however, appeared to be photoactivated as efficiently as Dronpa.

Because the two Dronpa mutants are highly sensitive to 490-nm light, we measured their excitation and emission spectra using fully photoactivated protein samples (Fig. 2). Based on the spectra, we calculated their fluorescence quantum yields ( $\phi_{FL}$ ). The  $\phi_{FL}$  values for Dronpa-2 and Dronpa-3 are 0.33 and 0.28, respectively.

In this study, we searched for new photoswitching kinetics by engineering the bright state of Dronpa to be more sensitive to blue light, while maintaining high quantum yields for fluorescence and photoactivation (D-to-B conversion). These features allow for an interesting fluorescence imaging modality. Illumination at 490 nm quickly decreases the population of the bright state, resulting in very faint fluorescence signals. On the other hand, illumination at 490 and 400 nm makes the proteins oscillate between their bright and dark states. In this situation, the bright state can be repetitively excited at 490 nm to induce the emission of green fluorescence.

Note that illumination at 400 nm does not produce a signal. Therefore, when 405-nm and 488-nm laser beams are coaxially introduced on a Dronpa-2 or Dronpa-3 labeled sample, bright fluorescence should be generated only at the focal

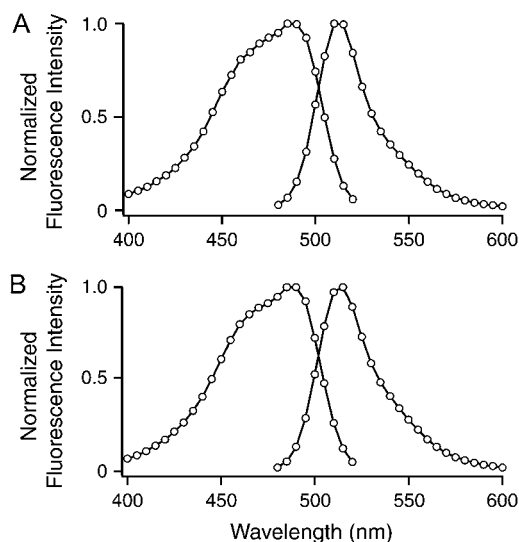


**FIGURE 2** Normalized excitation and emission spectra of Dronpa-2 (A) and Dronpa-3 (B). Protein samples were photoactivated using 400-nm light before measurements.

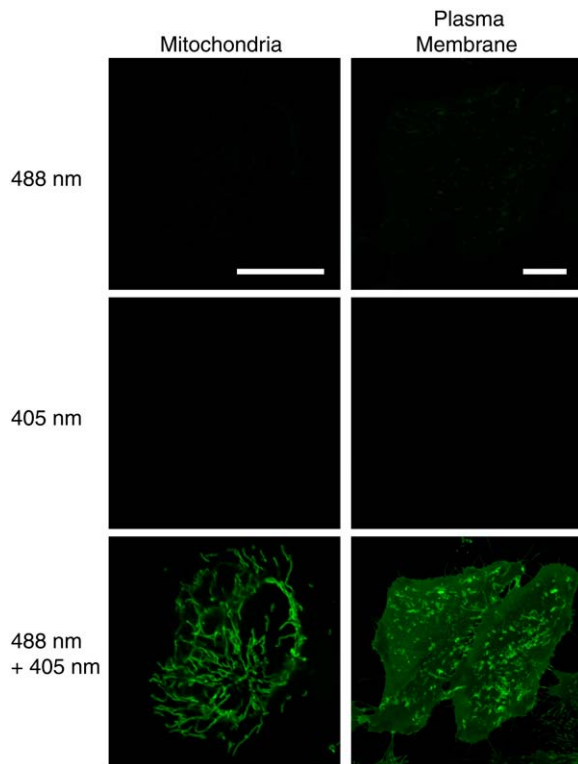


**FIGURE 3** Fluorescent images of HeLa cells expressing mitochondrially targeted (*left*) and plasma-membrane-targeted (*right*) Dronpa-3. Dronpa-3 was fused with the 12 N-terminal amino acids of the cytochrome *c* oxidase subunit IV presequence and the 22 N-terminal amino acids of the nonreceptor tyrosine kinase Lyn, respectively (8). 488 nm, images with a 488-nm laser scan; 405 nm, images with a 405-nm laser scan; 488 nm + 405 nm, images with a 488-nm and 405-nm laser scan. Scale bars, 10  $\mu$ m. Cells were visualized using a confocal microscope equipped with a 60 $\times$  objective lens (Plan Apo, NA = 1.40), a laser diode (405 nm), and an argon ion laser (488 nm) (Fluoview FV500, Olympus, Tokyo, Japan). Kalman averaging of four scans was performed on each scanning line.

point where intensities are high. To demonstrate this concept, we simultaneously illuminated Dronpa-3 with 405-nm and 488-nm lasers. We chose Dronpa-3 because it folded better in cultured cells than Dronpa-2. Dronpa-3 was targeted to mitochondria or to the plasma membrane of HeLa cells (Fig. 3). A laser scan at 405 nm or 488 nm did not produce detectable signals, but a simultaneous scan with both lasers highlighted the targeted subcellular structures. If the two lasers are aligned independently using separate objectives,

it should be possible to spatially restrict the generated fluorescence signal, which can be collected in a wide-field detection mode.

During preparation of this manuscript, a paper by Stiel et al., which reported similar Dronpa mutants with fast photoswitching (5) was published. Based on the crystal structure of Dronpa and its comparison with that of asFP595 (6), another reversibly photoswitchable fluorescent protein, the authors introduced mutations at Val<sup>157</sup> or Met<sup>159</sup>. They found that Dronpa-Val<sup>157</sup>Gly and Dronpa-Met<sup>159</sup>Thr exhibit faster and more reliable on-to-off transitions than the wild-type protein, and may be suitable for breaking the diffraction barrier of light microscopy using the reversible saturable optical transitions (RESOLFT) technique (7).

## ACKNOWLEDGMENTS

This work was partly supported by grants from the Molecular Ensemble Development Research, the Special Coordination Fund for the promotion of the Ministry of Education, Culture, Sports, Science, and Technology, the Japanese Government, the New Energy and Industrial Technology Development Organization, and the Human Frontier Science Program.

## REFERENCES and FOOTNOTES

1. Ando, R., H. Mizuno, and A. Miyawaki. 2004. Regulated fast nucleocytoplasmic shuttling observed by reversible protein highlighting. *Science*. 306:1370–1373.
2. Habuchi, S., R. Ando, P. Dedecker, W. Verheijen, H. Mizuno, A. Miyawaki, and J. Hofkens. 2005. Reversible photoswitching in the GFP-like fluorescent protein Dronpa. *Proc. Natl. Acad. Sci. USA*. 102:9511–9516.
3. Dedecker, P., J. Hotta, R. Ando, A. Miyawaki, Y. Engelborghs, and J. Hofkens. 2006. Fast and reversible photoswitching of the fluorescent protein dronpa as evidenced by fluorescence correlation spectroscopy. *Biophys. J.* 91:L45–L47.
4. Sawano, A., and A. Miyawaki. 2000. Directed evolution of green fluorescent protein by a new versatile PCR strategy for site-directed and semi-random mutagenesis. *Nucleic Acids Res.* 28:e78.
5. Stiel, A. C., S. Trowitzsch, G. Weber, M. Andresen, C. Eggeling, S. W. Hell, S. Jakobs, and M. C. Wahl. 2007. 1.8 Å bright-state structure of the reversibly switchable fluorescent protein Dronpa guides the generation of fast switching variants. *Biochem. J.* 402:35–42.
6. Lukyanov, K. A., D. M. Chudakov, S. Lukyanov, and V. V. Verkhusha. 2005. Innovation: photoactivatable fluorescent proteins. *Nat. Rev. Mol. Cell Biol.* 6:885–891.
7. Hell, S. W., M. Dyba, and S. Jakobs. 2004. Concepts for nanoscale resolution in fluorescence microscopy. *Curr. Opin. Neurobiol.* 14: 599–609.
8. Sawano, A., H. Hama, N. Saito, and A. Miyawaki. 2002. Multicolor imaging of Ca<sup>2+</sup> and protein kinase C signals using novel epifluorescence microscopy. *Biophys. J.* 82:1076–1085.